Analysis of Average Signal-to-Interference-Noise Ratio for Indoor UWB Rake Receiving System

Tao Jia and Dong In Kim
School of Engineering Science
Simon Fraser University, Burnaby, BC, V5A 1S6 Canada
E-mail: {tjia, dikim}@sfu.ca

Abstract— **In this paper, we derive an analytical expression for average signal-to-interference-plus-noise ratio (SINR) for ultra wideband (UWB) Rake receiver in an indoor multiuser communication scenario, given that the interference level is fluctuating due to asynchronous transmission among different users. The indoor wireless channel model adopted here is a standard channel model recently released by IEEE 802.15 study group 3a. We propose a theoretical framework to analyze the average SINR and show that our analysis is well coincident with the simulation results. Finally, we show that our result can be used to theoretically determine the optimum integration interval for a single-user UWB transmitted reference (TR) system.**

Keywords: Ultra wideband (UWB), average output SINR, lognormal distribution, double Poisson process

I. Introduction

Ultra wideband (UWB) technology has been proposed as a promising alternative for indoor wireless multiple-access communication systems to support short-range high data rate transmissions [1]-[2]. In [2], the authors analyzed the multiple-access performance of a time-hopping (TH) pulse position modulation (PPM) UWB system based on the Gaussian assumption of multiple-access interference (MAI). After that, [3] derived an exact BER expression using the characteristic function method and evaluated the accuracy of Gaussian assumption used in [2]. However, both papers only considered additive white Gaussian noise (AWGN) channel.

Recently, IEEE 802.15 study group 3a has accepted the indoor wireless channel model developed at Intel for UWB systems [4], in which the clustering of path arrivals was reported. Specifically, the multipath components arrive according to a double Poisson process and the fading coefficient of each multipath component has an independent lognormal distribution rather than Rayleigh distribution. Furthermore, the double-exponential model was found to be better fit for the power decay profile. Based on this channel model, [5] presented signal-to-noise ratio (SNR) and bit-error-rate (BER) performance for different types of Rake receivers. However, they only considered single-user transmission. Besides, the results are given in a semi-analytical way. In [6], the authors found the optimum integration interval by maximizing the average output SNR for a single-user UWB-TR system. However, the optimum value of integration interval is given through simulation.

In this paper, we are particularly interested in analyzing the performance of Partial or All Rake receivers in terms of average combined output SINR in a typical indoor multiuser environment. To this end, we propose a theoretical framework to derive an analytical expression for average combined output SINR based on IEEE 802.15.3a channel model and show that our analysis is well coincident with simulation result. Based on this framework, we can compare the performance of UWB Rake receiving system in different types of indoor wireless channels, using the analytical SINR as a performance measure. Another application of the theoretical framework developed in this paper is to theoretically determine the optimum integration interval for UWB-TR system. The rest of the paper is organized in the following way. Section II describes the signal and channel model. Section III specifies the receiver structure and mathematical model used to analyze the average combined output SINR. Numerical and simulation results are given in Section IV. Concluding remarks are given in Section V.

II. Signal and Channel Model

We consider TH-binary PPM (BPPM) as the signaling method. The transmissions from different users are assumed to be asynchronous. Each user is assigned a random time-hopping pattern to avoid catastrophic collision with others. The TH-BPPM signal is represented by [2]

$$s^{(\nu)}(t) = \sum_{j=-\infty}^{+\infty} \sqrt{E_w}\, w(t - jT_f - c_j^{(\nu)}T_c - \delta d^{(\nu)}_{\lfloor j/N_s \rfloor}) \quad (1)$$

where $w(t)$ is a unit-enery transmitted pulse and E_w is the transmitted pulse energy. δ represents the time shift associated with binary PPM modulation and $d^{(\nu)}$ is the user-specific data sequence. T_f is the frame time in which only one pulse is transmitted and N_s denotes the number of frames per symbol. $c_j^{(\nu)}$ is the time-hopping value for the jth frame of νth user and T_c is the chip duration.

The impulse response of the UWB channel model can be written as [4]

$$h(t)=\sum_{l=0}^{L}\sum_{k=0}^{K}\alpha_{k,l}\delta(t-T_l-\tau_{k,l}) \tag{2}$$

where $\alpha_{k,l}$ is the gain coefficient of the kth ray in lth cluster and $\tau_{k,l}$ is the arrival time of kth ray relative to lth cluster's arrival time T_l. The inter-cluster and inter-ray arrival times are independently exponentially distributed. Furthermore, $\alpha_{k,l}=p_{k,l}\beta_{k,l}$ where $p_{k,l}$ equiprobably takes on the values of ±1 accounting for the random pulse inversion that occurs due to reflections and $\beta_{k,l}$ is a lognormal random variable, denoted by $20\log_{10}(\beta_{k,l})\propto N(\mu_{k,l},\sigma^2)$. The power profile is double exponentially decaying, given by $\mathbf{E}\{\beta_{k,l}^2\}=\Omega_0\exp(-T_l/\Gamma)\exp(-\tau_{k,l}/\gamma)$ ($\mathbf{E}$ denotes the expectation), where Ω_0 is the mean power of the first ray of the first cluster, Γ and γ represent the power decay factors of the cluster and ray, respectively.

The signal received by the *desired* first user within one-symbol duration can be written as (assuming symbol 0 is transmitted by the first user)

$$\begin{aligned} r(t)=&\sum_{j=0}^{N_s-1}\sqrt{E_w}\,g^{(1)}(t-jT_f-c_j^{(1)}T_c) \\ +&\sum_{\nu=2}^{N_u}\sum_{j=-\infty}^{+\infty}\sqrt{E_w}\,g^{(\nu)}(t-jT_f-c_j^{(\nu)}T_c-\delta d_{\lfloor j/N_s\rfloor}^{(\nu)}-\tau_0^{(\nu)})\end{aligned} \tag{3}$$

where $g^{(\nu)}(t)=w(t)\otimes h^{(\nu)}(t), \nu=1,2,\ldots,N_u$ and N_u is the total number of users. $h^{(\nu)}(t)$ is the channel impulse response for νth user and $\otimes$ denotes convolution. $\tau_0^{(\nu)}$ represents νth user's reference delay relative to the first user caused by asynchronous transmission ($\tau_0^{(1)}=0$).

III. Rake Performance Analysis

We consider the discrete-time channel model for (2). The whole arrival time axis can be divided into time bins of $\Delta\tau$, in which one or more multipath components (MPC) arrive, or no arrival at all. Based on this model, we can rewrite (2) for νth user's channel impulse response as

$$h^{(\nu)}(t)=\sum_i A_i^{(\nu)}\delta(t-\tau_i) \tag{4}$$

where $\tau_i=(i-1)\Delta\tau$ is ith time bin and $A_i^{(\nu)}$ represents the sum of the channel coefficients of all MPCs arrived in ith time bin.

For the first user, assuming perfect timing synchronization, the output of ith Rake finger in the tapped-delay-line model is ($v(t)=w(t)-w(t-\delta)$)

$$Z_i=\sum_{j=0}^{N_s-1}\int_{\tau_i+jT_f}^{\tau_i+(j+1)T_f} r(t)v(t-jT_f-c_j^{(1)}T_c-\tau_i)\,dt \tag{5}$$

Given perfect channel estimation, the decision statistic after maximal-ratio combining (MRC) of the first L_p paths is expressed as

$$Z=\sum_{i=1}^{L_p}\sqrt{E_w}\,A_i^{(1)}Z_i \tag{6}$$

where $A_i^{(1)}$ represents the channel coefficient of ith time bin of the first user and is assumed to be known to the receiver. To avoid inter-frame interference, we assume

$$N_hT_c+T_m+T_w+\delta\le\frac{T_f}{2} \tag{7}$$

where N_hT_c corresponds to the maximum time-hopping shift, T_m is the channel delay spread, and T_w is the pulse width. Based on (7) and following the derivation in [2], the *instantaneous* output SINR conditioned on all the channel coefficients of all users can be formulated as

$$\mathrm{SINR}(\{A_n^{(\nu)}\})=\frac{\mathrm{S}^2}{\sigma_{\text{rec}}^2+E_w^2N_sT_f^{-1}\sum_{\nu=2}^{N_u}{G_{\text{eff}}^{(\nu)}}^2} \tag{8}$$

where the numerator is the desired signal energy and the denominator represents receiver noise plus MAI. The quantities S, σ_{rec}^2 and ${G_{\text{eff}}^{(\nu)}}^2$ are evaluated in Appendix A to be

$$\mathrm{S}=E_wN_sR(0)\sum_{i=1}^{L_p}{A_i^{(1)}}^2 \tag{9}$$

$$\sigma_{\text{rec}}^2=N_0N_sE_wR(0)\sum_{i=1}^{L_p}{A_i^{(1)}}^2 \tag{10}$$

$${G_{\text{eff}}^{(\nu)}}^2=\sum_{i=1}^{L_p}\sum_{k=1}^{L_p}\sum_{n=1}^{N_{\text{tot}}}\sum_{q=1}^{N_{\text{tot}}}A_i^{(1)}A_k^{(1)}A_n^{(\nu)}A_q^{(\nu)}Q[(i-k-n+q)\Delta\tau] \tag{11}$$

where $R(\cdot)$ represents the correlation function between the received pulse $w(t)$ and template signal $v(t)$. $N_0/2$ is the double-side power spectral density of AWGN. N_{tot} is the total number of time bins to be considered for each channel realization. $Q(\cdot)$ is defined as the autocorrelation function of $R(\cdot)$.

To find *channel-averaged* SINR, which is defined by

$$\begin{aligned}\mathrm{SINR}&\triangleq\mathbf{E}\{\mathrm{SINR}(\{A_n^{(\nu)}\})\} \\ &=\frac{\left|\mathbf{E}\{\mathrm{S}\}\right|^2}{\mathbf{E}\{\sigma_{\text{rec}}^2\}+E_w^2N_sT_f^{-1}\sum_{\nu=2}^{N_u}\mathbf{E}\{{G_{\text{eff}}^{(\nu)}}^2\}},\end{aligned} \tag{12}$$

we need to take another expectation with respect to channel. Considering the interference part (i.e., MAI), we need to calculate $\mathbf{E}\{{G_{\text{eff}}^{(\nu)}}^2\}$. For a specific channel realization, we have $A_n^{(\nu)}=\sum_u p_{n,u}^{(\nu)}\beta_{n,u}^{(\nu)}$ and $A_q^{(\nu)}=\sum_w p_{q,w}^{(\nu)}\beta_{q,w}^{(\nu)}$, where $(p_{n,u}^{(\nu)}, p_{q,w}^{(\nu)})$ equiprobably take on the values of ±1 and $(\beta_{n,u}^{(\nu)}, \beta_{q,w}^{(\nu)})$ represent uth and wth MPC arrived in nth and qth time bins, respectively. Note that there is some difference between the definition for the subscripts of $\beta_{n,u}^{(\nu)}$ and that of $\beta_{k,l}$ in (2). Due to the independency between different MPCs and the fact that $\mathbf{E}\{p_{n,u}^{(\nu)}\} = 0$ and $\mathbf{E}\{{p_{n,u}^{(\nu)}}^2\} = 1$, we have

$$\mathbf{E}\{A_n^{(\nu)} A_q^{(\nu)}\} = \begin{cases} \mathbf{E}\{{A_n^{(\nu)}}^2\} = \sum_u \mathbf{E}\{{\beta_{n,u}^{(\nu)}}^2\}, & n = q \\ 0, & n \neq q. \end{cases} \tag{13}$$

Note that (13) also holds for the first user. Using this result, the expectation of (11) will have nonzero components only when $i = k$ and $n = q$, leading to

$$\mathbf{E}\{{G_{\text{eff}}^{(\nu)}}^2\} = Q(0) \cdot \sum_{i=1}^{L_p} \mathbf{E}\{{A_i^{(1)}}^2\} \cdot \sum_{n=1}^{N_{\text{tot}}} \mathbf{E}\{{A_n^{(\nu)}}^2\}. \tag{14}$$

Substituting (14) into (12), the *channel-averaged* SINR can be formulated as

$$\text{SINR} = \frac{E_w N_s R(0)^2 \sum_{i=1}^{L_p} \mathbf{E}\{{A_i^{(1)}}^2\}}{N_0 R(0) + E_w Q(0) T_f^{-1} \sum_{\nu=2}^{N_u} \sum_{n=1}^{N_{\text{tot}}} \mathbf{E}\{{A_n^{(\nu)}}^2\}}. \tag{15}$$

The computation of (15) requires the evaluation of average path energy. Recalled our discrete-time channel model, there could be MPC arrival or not in any given time bin. Starting from here and throughout the whole paper, when we mention a *cluster arrival* in any given time bin, we actually refer to the arrival of the first ray component within this cluster. Accordingly, a *ray arrival* is always referring to the arrival of a ray component other than the first one within each cluster.

Assuming $\Delta\tau$ is small enough, say 0.167ns in [4], it is well known that Poisson arrival process can be approximated by Binomial distribution. Specifically, there could be one or no cluster arrival in $\Delta\tau$ with the probabilities given by $P_c \triangleq \Lambda\Delta\tau$ and $1 - P_c$, respectively. In addition, given a cluster arrival in a certain time bin, there could be one or no ray arrival in any following time bin with the probabilities given by $P_r \triangleq \lambda\Delta\tau$ and $1 - P_r$, respectively ($1/\Lambda$ and $1/\lambda$ are defined as the cluster and ray arrival rates, respectively). The probability that there are more than one *cluster arrival* in $\Delta\tau$ is zero. Similarly, within the same cluster, the probability that there are more than one *ray arrival* in $\Delta\tau$ is also zero.

Based on the above assumption, there could only be a *finite number* of arrival patterns in each time bin. Specifically, consider $\tau_n = (n-1)\Delta\tau$, we can identify two disjoint events such as $I \triangleq \{\text{at least one MPC arrives at } \tau_n\}$ and $\bar{I} \triangleq \{\text{no MPC arrives at } \tau_n\}$. Since $\mathbf{E}\{{A_n^{(\nu)}}^2\} = 0$ when no MPC arrives at τ_n, we have

$$\mathbf{E}\{{A_n^{(\nu)}}^2\} = \mathbf{E}\{{A_n^{(\nu)}}^2 \,|\, I\} P(I). \tag{16}$$

In the evaluation of average path energy, we find the following lemma useful.

Lemma: The probability that mth ($m = 1, 2, \ldots, n-1$) time bin has a ray contribution to nth ($n > 1$) time bin τ_n, denoted by $P_m^{(n)}$, can be calculated in two cases:

$$P_m^{(n)} = \begin{cases} P_r, & m = 1 \\ P_c \cdot P_r, & 2 \leq m \leq n-1. \end{cases} \tag{17}$$

Proof of this lemma can be found in Appendix B. It indicates the probability that mth time bin has a ray contribution to nth time bin can be simply calculated as the joint probability that a cluster arrives at mth time bin and this cluster results in a ray at nth time bin.

Using this lemma and listing all possible arrival patterns in nth time bin, the average path energy is derived as (see Appendix C)

$$\mathbf{E}\{{A_n^{(\nu)}}^2\} = \begin{cases} \Omega_0, & \text{for } n = 1 \\ \Omega_0 P_c \exp\left[-\frac{(n-1)\Delta\tau}{\Gamma}\right] + \Omega_0 P_r \exp\left[-\frac{(n-1)\Delta\tau}{\gamma}\right] \\ \quad + \Omega_0 P_c P_r \exp\left[-\frac{n\Delta\tau}{\gamma} + \frac{\Delta\tau}{\Gamma}\right] \frac{\rho^2(1-\rho^{n-2})}{1-\rho}, & \text{for } n \geq 2 \end{cases} \tag{18}$$

where $\rho = \exp\left(\frac{\Delta\tau}{\gamma} - \frac{\Delta\tau}{\Gamma}\right)$. Note that the user-specific superscript ν has been omitted for notational simplicity. It should be pointed out that, by defining $\bar{E}_c^{(\nu)} \triangleq \mathbf{E}\{\sum_{n=1}^{N_{\text{tot}}} {A_n^{(\nu)}}^2\} = \mathbf{E}\{\sum_{l=1}^{L} \sum_{k=1}^{K} |\alpha_{k,l}^{(\nu)}|^2\}$, we can now theoretically set

$$\Omega_0^{(\nu)} = \frac{1}{\bar{E}_0^{(\nu)}} \triangleq \frac{1}{\bar{E}_c^{(\nu)}|_{\Omega_0^{(\nu)}=1}} \tag{19}$$

so as to make $\bar{E}_c^{(\nu)} = 1$ (normalized), instead of normalizing the total channel energy for each realization as suggested in [4]. By selecting the corresponding $\Omega_0^{(\nu)}$ for each user and substituting (18) into (15), the *channel-averaged* output SINR is derived as

$$\begin{aligned} \text{SINR} = & \frac{E_w N_s R(0)^2 \Omega_0^{(1)}}{N_0 R(0) + E_w Q(0) T_f^{-1} (N_u - 1)} \\ & \times \left[1 + P_c \frac{\exp\left(-\frac{\Delta\tau}{\Gamma}\right) - \exp\left(-\frac{L_p\Delta\tau}{\Gamma}\right)}{1 - \exp\left(-\frac{\Delta\tau}{\Gamma}\right)} \right. \\ & + P_r \frac{\exp\left(-\frac{\Delta\tau}{\gamma}\right) - \exp\left(-\frac{L_p\Delta\tau}{\gamma}\right)}{1 - \exp\left(-\frac{\Delta\tau}{\gamma}\right)} \\ & + P_c P_r \frac{\rho^2 \exp\left(\frac{\Delta\tau}{\Gamma}\right)}{1-\rho} \left[\frac{\exp\left(-\frac{2\Delta\tau}{\gamma}\right) - \exp\left(-\frac{(L_p+1)\Delta\tau}{\gamma}\right)}{1 - \exp\left(-\frac{\Delta\tau}{\gamma}\right)} \right. \\ & \left.\left. - \frac{\exp\left(-\frac{2\Delta\tau}{\gamma}\right) - \rho^{L_p-1} \exp\left(-\frac{(L_p+1)\Delta\tau}{\gamma}\right)}{1 - \exp\left(-\frac{\Delta\tau}{\Gamma}\right)} \right] \right]. \end{aligned} \tag{20}$$

IV. Integration Interval Optimization for UWB-TR System

A direct application of the theoretical framework developed here is to determine the optimum integration interval for a single-user UWB-TR system, in which the average output SNR(L_p) can be derived as a function of integration interval via L_p, formulated as

$$\text{SNR}(L_p) = \frac{N_s E_w^2 R_w^2(0)\big[G^{(1)}(L_p)\big]^2}{E_w N_0 R_w(0) G^{(1)}(L_p) + L_p N_0^2/2} \tag{21}$$

where $G^{(1)}(L_p) \triangleq \sum_{i=1}^{L_p} \mathbf{E}\{{A_i^{(1)}}^2\}$ and $R_w(\cdot)$ denotes the autocorrelation of transmitted pulse. By substituting (18) into (21), we can numerically find the optimum integration interval given by

$$L_p^{\text{opt}} = \text{argmax}\big\{\text{SNR}(L_p)\big\} \tag{22}$$

which is a function of channel parameters, transmit power, noise power as well as pulse-specific parameter.

V. Results

To validate our theoretical framework in Section III, we choose $N_{\text{tot}} = 200$ and $\Delta\tau = 0.167$ns for our analysis as well as simulation and then $\bar{E}_0^{(\nu)}$ is calculated accordingly. Without considering the long-term lognormal shadowing, $\bar{E}_0^{(\nu)}$ for CM1, CM2, CM3 and CM4 are shown in Table I.

TABLE I
AVERAGE CHANNEL ENERGY FOR 4 TYPES OF INDOOR CHANNEL MODEL

$\bar{E}_0^{(\nu)}$	CM1	CM2	CM3	CM4
$N_{\text{tot}} = 200$	13.3837	13.4105	30.2707	48.0312
N_{tot} enough	13.4297	13.6438	33.5808	67.5412

In Table I, we also calculated the average path energy when N_{tot} is large enough for each type of channel as suggested in [4], i.e. $N_{\text{tot}} = \lfloor 10(\Gamma+\gamma)/\Delta\tau \rfloor$. As we can see, when $N_{\text{tot}} = 200$, we captured most of the channel energy.

In our simulation, we assume that all 20 users experience the same type of channel model and transmit the third-order derivative Gaussian pulse with unit energy $E_w = 1$. The frame time is $T_f = 90$ns and the pulse repetition is $N_s = 1$. Fig. 1 shows the average output SINR versus the number of Rake fingers in CM1 and CM3. We can see that our analysis well matches with the simulation results. The discrepancies occurring for a small number of Rake fingers are mainly due to that the 0.167ns time bin is not small enough to well approximate Poisson process with a Binomial distribution. As observed in our simulations, the discrepancies become less when smaller $\Delta\tau$ is adopted.

Fig. 2 presents the numerical results for optimum integration interval determined by (22), from which we can see, for each type of channel model, there exists an optimum integration interval that maximizes the average output SNR. Using the same parameters except $N_{\text{tot}} = \lfloor 10(\Gamma+\gamma)/\Delta\tau \rfloor$ for normalization, L_p^{opt} is found to be $9.0\text{ns}, 16.9\text{ns}, 22.5\text{ns}$, and 40.4ns for CM1 to CM4, respectively. Furthermore, the maximum average output SNR corresponding to the optimum integration time can be used as an upper limit for multiuser UWB-TR system.

VI. Conclusion

In this paper, we have derived an analytical expression for average output SINR under IEEE 802.15.3a channel model. The theoretical framework developed here can be used to compare the average output SINR as a useful performance measure for UWB Rake receiving system under different indoor channel models. Another benefit from this framework is we can theoretically determine the optimum integration interval with corresponding maximum average output SNR for a single-user UWB TR system, which will be a promising scheme for UWB signaling.

Appendix A
Derivation of Instantaneous Output SINR

Using (3) and (5), we can write the ith Rake finger output Z_i as a sum of three terms, denoted by

$$Z_i = Z_i^S + Z_i^I + Z_i^N \tag{23}$$

where the three terms representing desired signal, MAI and noise components are derived as [2]

$$Z_i^S = \sqrt{E_w} N_s R(0) A_i^{(1)} \tag{24}$$

$$Z_i^I = \sqrt{E_w} \sum_{\nu=2}^{N_u} \sum_{j=0}^{N_s-1} \sum_{n=1}^{N_{\text{tot}}} A_n^{(\nu)} R\bigg((c_j^{(1)} - c_{j+j_\nu}^{(\nu)}) T_c - \delta d_{\lfloor (j+j_\nu)/N_s \rfloor}^{(\nu)} + \alpha_\nu + \tau_i^{(1)} - \tau_n^{(\nu)} \bigg) \tag{25}$$

$$Z_i^N = \sum_{j=0}^{N_s-1} \int_{\tau_i^{(1)}+jT_f}^{\tau_i^{(1)}+(j+1)T_f} n(t) v(t - jT_f - c_j^{(1)} T_c - \tau_i^{(1)})\, dt \tag{26}$$

In (25), α_ν and j_ν have similar definitions as in [2]. After combining the first L_p Rake fingers in the fashion of MRC shown by (6), the decision statistic can be written as

$$Z = \underbrace{E_w N_s R(0) \sum_{i=1}^{L_p} {A_i^{(1)}}^2}_{\text{S}} + \underbrace{\sum_{\nu=2}^{N_u} n^{(\nu)} + n_{\text{rec}}}_{n_d} \tag{27}$$

where $n^{(\nu)}$ and n_{rec} represent MAI and noise, respectively and their expressions are omitted due to limited space. We can prove that $n^{(\nu)}$, $\nu = 2, 3, \ldots, N_u$ and n_{rec} have zero-mean and are independent of each other. Hence, we have

$$\mathbf{E}\{{n_d}^2\} = \sum_{\nu=2}^{N_u} \mathbf{E}\{{n^{(\nu)}}^2\} + \mathbf{E}\{{n_{\text{rec}}}^2\}. \tag{28}$$

It is easy to show that $\sigma_{\text{rec}}^2 = \mathbf{E}\{{n_{\text{rec}}}^2\}$ has the expression show by (10). Following the derivation in [2] and defining $Q(x) = \int_{-\infty}^{\infty} R(\tau + x)R(\tau)d\tau$, we will get (11) and finally obtain (8) by substituting all terms calculated above.

Appendix B
Probability of mth Time Bin Contributing a Ray to nth Time Bin

Case 1: for $m = 1$, we always have the first cluster ($l = 0$) arrived in the first time bin. The probability that this cluster has a ray contribution to nth time bin is calculated to be

$$\begin{aligned} P_1^{(n)} &= \sum_{k=1}^{n-1} P[\tau_{k,0} = (n-1)\Delta\tau] \\ &= \sum_{k=1}^{n-1} P_r \binom{n-2}{k-1} P_r^{k-1}(1-P_r)^{n-k+1} \\ &= P_r. \end{aligned} \tag{29}$$

Case 2: for $2 \le m \le n-1$, the probability that mth time bin has a ray contribution to nth time bin can be derived in a similar way as

$$\begin{aligned} P_m^{(n)} &= \sum_{l=1}^{m-1} P[T_l = (m-1)\Delta\tau] \sum_{k=1}^{n-m} P[\tau_{k,l} = (n-m)\Delta\tau] \\ &= P_c \cdot P_r. \end{aligned} \tag{30}$$

Appendix C
Evaluation of Average Path Energy

Consider the first cluster in the first time bin ($\tau_1 = 0$), we have

$$\mathbf{E}\{{A_1^{(\nu)}}^2\} = \Omega_0. \tag{31}$$

For the time bins other than the first one, I could be divided into only two kinds of possible arrival patterns. One is a cluster plus $N_r\,(N_r = 0, 1, \ldots, n-1)$ rays, the other is no cluster but $N_r\,(N_r = 1, \ldots, n-1)$ rays. In other words, at most $n-1$ preceding clusters can arrive before τ_n and the maximum ray arrival within τ_n caused by all preceding clusters can not exceed $n-1$. Classifying the above two arrival patterns as I_1 and I_2, respectively, (16) can be rewritten as

$$\mathbf{E}\{{A_n^{(\nu)}}^2\} = \mathbf{E}\{{A_n^{(\nu)}}^2 \,|\, I_1\}P(I_1) + \mathbf{E}\{{A_n^{(\nu)}}^2 \,|\, I_2\}P(I_2). \tag{32}$$

By specifying the probabilities for all the possible arrival patterns, we can calculate the average path energy associated with each event and finally get (18) by adding them together.

Acknowledgment

This research was supported in part by the Ultra Wideband Wireless Communications Research Center of Inha University.

References

[1] M. Z. Win and R. A. Scholtz, "Impulse radio: How it works," *IEEE Commun. Letters*, vol. 2, pp. 36–38, Feb. 1998.

[2] M. Z. Win and R. A. Scholtz, "Ultra-wide bandwidth time-hopping spread-spectrum impulse radio for wireless multiple-access communications," *IEEE Trans. Commun.*, vol. 48, pp. 679–691, Apr. 2000.

[3] B. Hu and N. C. Beaulieu "Accurate evaluation of multiple access performance in TH-PPM and TH-BPSK," *IEEE Proc. ICC '04*, vol. 1 pp. 300–305 June 2004.

[4] IEEE P802.15-02/368r5-SG3a, "Channel Modeling Sub-committee Report Final", November 18, 2002.

[5] A. Rajeswaran, V. S. Somayazulu and J. R. Foerster, "Rake performance for a pulse based UWB system in a realistic UWB indoor channel," *IEEE Proc. ICC '03*, vol. 4, pp. 2879–2883 May 2003.

[6] S. Franz and U. Mitra, "Integration Interval Optimization and Performance Analysis for UWB Transmitted Reference Systems," *Joint UWBST & IWUWBS, International Workshop on*, pp. 26–30 May 2004.

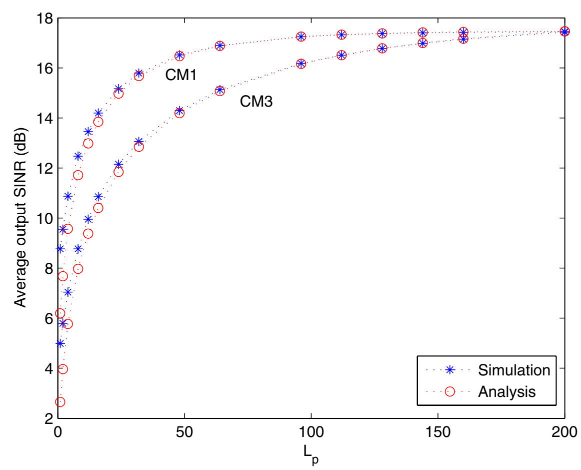

Fig. 1. Average output SINR versus number of Rake fingers for CM1 and CM3 channel models when $N_s = 1$ and $E_b/N_0 = 18$dB.

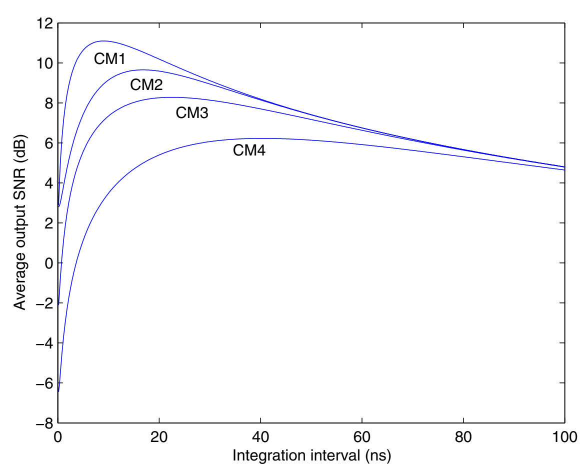

Fig. 2. Average output SNR versus integration time for 4 different channel models when $N_s = 1$ and $E_b/N_0 = 15$ dB.